Influence of Preparation Processing on the Transport Properties of Melt-Spun Sb2–xBixTe3+y

Viktoriia Ohorodniichuk, Christophe Candolfi, Masschelein Philippe, Philippe Baranek, Pascal Dalicieux, Anne Dauscher, Bertrand Lenoir

Influence of the preparation processing on the transport properties of melt-spun $Sb_{2-x}Bi_xTe_{3+y}$

V. Ohorodniichuk[1,2], C. Candolfi[1], Ph. Masschelein[1], Ph. Baranek[2],

P. Dalicieux[2], A. Dauscher[1], B. Lenoir[1]

[1] Institut Jean Lamour, CNRS – Université de Lorraine, Parc de Saurupt, F-54011 NANCY Cedex, France

[2] EDF R&D, Site des Renardières, Avenue des Renardières – Ecuelles 77818 Moret-sur-Loing Cedex, France

E-mail of corresponding author: viktoriia.ohorodniichuk@univ-lorraine.fr

Telephone of corresponding author: +33 3 83 58 41 76

In this work, we present our attempt to improve the thermoelectric performance of melt-spun (MS) $Sb_{2-x}Bi_xTe_{3+y}$ samples densified by Spark Plasma Sintering (SPS) through two different methods: 1) alignment of the MS ribbons in the SPS die; 2) repetitive SPS sintering. Microstructural study of the dense samples was performed by scanning electron microscopy supported by X-ray diffraction analyses. The thermoelectric and galvanomagnetic properties were measured in the direction perpendicular to the uniaxial pressing direction of SPS. Alignment of the ribbons gives rise to improved thermoelectric performances with an increase of up to 26% with respect to the reference sample yielding a peak dimensionless figure of merit *ZT* value of 1.1 at 355 K. Yet, in contrast to recent studies, we observed a decrease in the thermoelectric efficiency of ~10% in the $Sb_{1.5}Bi_{0.5}Te_{3.1}$ sample prepared by double-SPS compared to the sample densified with a single SPS process. Nevertheless, all MS samples possess improved thermal and electrical properties compared to the reference samples, proving the positive influence of this method.

Key words: Bismuth antimony telluride, melt-spinning, spark plasma sintering, thermoelectric properties, SEM.

Introduction

Since the early 50^{ties} of the last century, ternary systems based on solid solutions of Sb_2Te_3 and Bi_2Te_3 are known as the most promising *p*-type materials for thermoelectric devices operating in the temperature range 200 – 400 K. After the rapid improvement of *ZT* values from 0.3 to about 1.0 in the 1970s, it seemed that the limit was

reached and the general interest to the subject was receding in the following decades. The development of nanostructures in the beginning of 1990s brought new ideas and new hopes to scientists. Different approaches based on top-down or bottom-up methods were implemented to obtain nano-structured thermoelectric materials. Among them, the melt-spinning method applied to the Bi_2Te_3 family of compounds, used for room temperature applications, led to unprecedented results [1, 2].

The melt-spinning technique is not a newcomer in the field of material science, being known from the beginning of 1900, but was mostly used for the preparation of amorphous metallic ribbons. To the best of our knowledge, the first report [3] on the application of melt-spinning to thermoelectric materials was published in 1986. This work, applied to the binary Bi_2Te_3 compounds, neither received any resonance in the field, nor new attempts made on ternary (Bi,Sb,Te) compositions some years later [4]. It was only in late 2000s that several papers claimed that the melt-spinning method combined with spark plasma sintering (SPS) densification can break the *ZT* barrier of 1.0 in $(Bi,Sb)_2Te_3$ alloys with *ZT* values as high as 1.6 near 300 K [1, 2].

The SPS, also known as field assisted sintering technique (FAST) or pulsed electric current sintering (PECS), uses Joule effect for the densification. Due to the joint actions of uniaxial pressure and pulsed electrical current, the process takes only few minutes to obtain a material of high density, making this approach unique in terms of time-saving. Moreover, the very short sintering time offers the opportunity to retain very fine microstructures and to prevent grain growth, rendering this technique essential for the preparation of nano-structured materials [5-10].

Belonging to the $R\bar{3}m$ space group, the $Sb_{2-x}Bi_xTe_{3+y}$ family of materials exhibits anisotropic physical properties due to the layered hexagonal (rhombohedral) structure. Thus, this feature suggests that arrangements of the grains in a preferable direction (texturing) may improve the transport properties of the samples. The idea of checking the influence of an additional structuration on the thermoelectric properties of materials was successfully realized by Kenfaui et al. [11] for cobaltite oxides. Repetitive SPS processes improved the texture of the sample and oriented the grains in a preferable way thereby resulting in a twofold increase in the *ZT* values. It was further applied with some promising results to *p*-type BiSbTe and *n*-type BiSeTe-based compounds prepared by mechanical alloying [12, 14]. So far, these approaches were not applied to the melt-spun (MS) samples and are thus worthwhile exploring.

Experimental procedures

To prepare initial ingots of a given nominal composition, basic elements of high purity (bismuth, antimony and tellurium (5N +, 99.999%)) were used in the form of granules. Stoichiometric amounts of these elements were placed in acid-cleaned and degased quartz tubes which were maintained under secondary vacuum for three hours before sealing. The final ingots were obtained by quenching the tubes in a water bath after having been heated up to 710°C during 5 hours in a vertical oscillating furnace. Each ingot was used both to prepare a reference sample in which no influence of nanostructuring is expected, and as the starting material for the melt-spinning process. The reference samples were obtained from densification by SPS of the grinded ingot applying a pressure of 30 MPa at 500 K. The melt-spun samples were prepared by densification of the ribbons under similar conditions. The ribbons were obtained by melt-spinning the ingot at 620°C on a cupper wheel of ø19.8 cm rotating at 36 m/s linear speed using an overpressure of 0.8 bar. An attempt to control the texturing of the MS samples was performed in two directions.

In the first approach, we prepared two $Sb_{1.48}Bi_{0.52}Te_3$ SPS samples from the same melt-spinning process. The first sample, further called grinded sample hereafter, was obtained from grinded ribbons densified by SPS in a 10 mm in diameter graphite die (Fig. 1a) whereas the second sample, further called aligned sample hereafter, was prepared from staked ribbons placed manually one by one in the die perpendicularly to the uniaxial pressure of SPS (Fig. 1b). In the second approach, we performed two cycles of SPS densification of the grinded $Sb_{1.5}Bi_{0.5}Te_{3.1}$ MS ribbons with the same heating ratio and pressure applied. For this purpose, a SPS densified pellet of 12 mm in diameter was placed in a die of 15 mm in diameter. A second SPS process was then applied in order to obtain a "double SPS" sample that was compared to the reference sample and to the MS sample prepared by a single SPS densification in the 12 mm die.

All consolidated samples have relative densities higher than 96% of the theoretical density. Powder X-ray diffraction (PXRD) patterns of the bulk samples were recorded on a Bruker D8 Advance diffractometer using CuKα1 radiation. Scanning electron microscopy (SEM) (XL30 FEG, Philips/FEI) was used to check the microstructural features. Transport properties measurements were performed on well-shaped samples cut from the consolidated ingots with a diamond-wire saw. The thickness of the bulk samples after SPS process varies in the range of 6-7 mm with diameter 10, 12 or 15 mm according to the experiment, allowing cutting square samples with a side of 6 mm

and about 1 mm in thickness for thermal diffusivity measurements in order to obtain values for the direction perpendicular to the uniaxial pressing direction. The bar-shaped samples for the low-temperature and high-temperature measurements, with cross section of about 2.5x2.5 mm and 7-8 mm length, were cut from the same materials. Low-temperature measurements of Seebeck coefficient (S), thermal conductivity (κ), electrical resistivity (ρ) as well as Hall carrier concentration (p) and Hall mobility (μ_H) were performed between 5 and 310 K using a physical property measurement system (PPMS, Quantum Design). S and ρ were measured simultaneously in the range 320 – 460 K with a ZEM-3 system (Ulvac-Rico). Thermal conductivity in the same range of temperatures was determined from thermal diffusivity (d) measurements (LFA 427, Netzsch) via the formula $\kappa = d \cdot c_p \cdot \rho$ where c_p is the specific heat and ρ is the density of the SPS samples considered to be temperature-independent. All physical properties were measured perpendicular to the direction of uniaxial pressing of SPS since it is in this direction that the thermoelectric properties are the best. For sake of completeness, we further probe the thermal conductivity at high temperature in the direction parallel to the pressing direction.

The experimental uncertainty in the determination of the thermal conductivity is estimated to ~ 8% at high temperatures. Similarly, the experimental uncertainty for both the electrical resistivity and thermopower are estimated to ~ 7%. Hence, the ZT values at temperatures above 300 K are determined with a combined experimental uncertainty of about 15-20%.

Results and discussion

Figure 2 shows the PXRD patterns obtained for the aligned and grinded MS-SPS samples collected on the polished surface perpendicular (Fig. 2a) and parallel (Fig. 2b) to the applied pressure. The one-SPS and double-SPS samples were studied in the same way (Fig. 3). All diffraction peaks correspond to the rhombohedral $Sb_{2-x}Bi_xTe_3$-structure. The comparison of intensity ratio of the (0.0.9) and (1.1.0) diffraction peaks was performed similarly to the study of Xie et al. [13]. The ratios of the grinded sample for the parallel and perpendicular directions were quite close ($I_{0.0.9}/I_{1.1.0}$ was equal to 0.17 and 0.18, respectively), while for the aligned sample, the increased texturing was found to be higher in the perpendicular direction ($I_{0.0.9}/I_{1.1.0}$ = 0.25 compared to 0.12 in the parallel direction). In the one-SPS sample, we obtained 0.16 and 0.17 for the parallel and perpendicular directions, respectively, which is coherent with the grinded sample since the same preparation method was used. On other hand, the double-SPS

sample also shows an enhanced structuring, but in the parallel direction (0.27 to the 0.15 for the perpendicular direction).

SEM investigations were carried out in order to identify structural features of the samples. Figure 4 shows the influence of grinding and alignment of MS ribbons on the orientation of crystal grains in dense SPS samples. The overall structure of the aligned sample appears denser with larger grains, although the lamellar structures are randomly oriented. SEM images of single and double-SPS samples are shown in Figure 5. The average grain size is lowered, but no evidence of improved structuration or preferred orientation can be found in the PXRD data.

Figure 6 shows the comparison between the transport properties measured on the grinded, aligned and reference samples. Both the aligned and grinded samples exhibit higher electrical resistivity values than the reference sample. Hall effect measurements indicate that these samples possess lower hole concentrations in agreement with the higher thermopower values measured. The decrease in the total thermal conductivity observed mainly reflects a decrease in the electronic contribution due to the higher electrical resistivity values. However, if we calculate the anisotropy factor defined as $I_{ani} = \frac{\kappa_{perp} - \kappa_{par}}{\kappa_{par}}$ [13], where κ_{perp} is thermal conductivity measured in the direction perpendicular to the pressing direction and κ_{par} – parallel to the pressing direction, we obtained that I_{ani} of the grinded sample is varying within the range of 0-1% while I_{ani} of the aligned sample is in the range of 21-25%. These results are in agreement with the above-mentioned PXRD texturing study. While the alignment of the ribbons has only a small positive effect on the thermoelectric performance with respect to the grinded sample, an overall increase of 26% with respect to the reference sample is observed with a peak *ZT* value of 1.1 at 355 K. We further note that no significant changes in the hole concentration are observed between the two modes of preparation suggesting that the deformation during the grinding step has no impact on the hole density.

Figure 7 presents the transport and galvanomagnetic properties measured on single, double-SPS and reference samples. The reduction in the electrical resistivity (about 12% with respect to the single-SPS sample) observed for the double-SPS sample can be linked to the improved orientation of the grains, thereby decreasing the number of grain boundaries perpendicular to the pressing direction, as already shown by Lognoné et al. [14]. On the other hand, the hole density was increased during the second SPS process by about 14%, reaching 2.8×10^{19} cm^{-3} at 300 K that directly contributes to the decrease in the electrical resistivity. Yet, this reduction does not compensate the increase in the total thermal conductivity from 1 W/K.m to 1.2 W/K.m for the double-SPS sample at 355 K. The anisotropy factor for the one-SPS sample is varying from 0 to 1% and for the double-SPS sample between 18 and 22%, which is

in a good agreement with the comparison of the PXRD peaks intensities. Thus, it seems from these results, that the double SPS approach is not a fruitful way of research to be pursued since an overall decrease in the *ZT* values by ~10% is observed. This result contrasts with that obtained in *n*-type Bi_2Te_3-Bi_2Se_3 materials [12, 14-15] for which the reported improvement was spectacular (40 – 50 %).

We stress here that the compositions based on Sb_2Te_3 or Bi_2Te_3 are known to deviate from the ideal stoichiometry, thereby creating numerous dislocations of atoms, antisite defects, vacancy or interstitial defects in the sample during the synthesis. Regarding the variation in the carrier concentration of the samples, we can state that each heat treatment of our materials is able to change the concentration of local defects. It was already shown in single-crystals that varying the saturation temperature results in significant changes in the charge carrier concentrations [16].

Further, we note that the melt-spinning approach is in general quite successful when comparing MS samples to the reference sample. The peak *ZT* values for the MS samples shift closer to room temperature (355 K) while reference samples exhibit the highest *ZT* values at higher temperatures (385 K). Despite being unable to reach extremely high *ZT* values, which were claimed in other articles [1, 2], we systematically observed an improvement of the thermoelectric figure of merit by about 18 – 20% in average compared to the samples that did not undergo MS procedure, in agreement with results obtained in recent investigations [17].

Conclusions

In this work, two different approaches were applied during SPS densification of the melt-spun ribbons of $Sb_{2-x}Bi_xTe_{3+y}$. The substitution of the grinding process of MS ribbons by their alignment in the SPS die has been performed in one set of samples of $Sb_{1.48}Bi_{0.52}Te_3$. Another set of $Sb_{1.5}Bi_{0.5}Te_{3.1}$ samples was exposed to repetitive densification by SPS. All approaches gave highly dense samples (over 96% of theoretical density), which were studied by XRD and SEM experiments. Though no structural changes were found, slight changes in transport and galvanomagnetic properties were observed. The alignment of the ribbons improved the *ZT* values by 26% over the reference sample, reaching 1.1 at 355 K through the decrease in the total thermal conductivity. The double-SPS process increases the carrier concentration of the sample but influences disadvantageously the thermal conductivity.

Thus, an overall decrease in the thermoelectric figure of merit by about 10% was found after the second SPS process. These results highlight the sensitivity of the transport properties of MS samples to the preparation process.

Acknowledgments

This work was performed with the sponsorship of Electricité de France R&D through the CIFRE convention N° 2011/1329.

References

1. W. Xie, X. Tang, Y. Yan, Q. Zhang, T.M. Tritt, J. Appl. Phys. 105, 113713 (2009).

2. Sh. Fan, J. Zhao, J. Guo, Q. Yan, J. Ma, H.H. Hng, Appl. Phys. Lett. 96, 182104 (2010).

3. V.M. Glazov, I.V. Yatmanov, A.B. Ivanova, Inorg. Mater. USSR 22, 596 (1986).

4. E. Koukharenko, N. Frety, V.G. Shepelevich, J.C. Tedenac, MRS Proceed. 545, 507 (1998).

5. S. Katsuyama, H. Okada, J. Jpn Soc. Powder & Powder Metal. 54, 375 (2007).

6. C.H. Kuo, M.S. Jeng, J.R. Ku, S.K. Wu, Y.W. Chou, C.S. Hwang, J. Elec. Mater. 38, 1956 (2009).

7. J. F. Li, J. Liu, Phys. Stat. Sol. (A) 203, 3768 (2006).

8. W.-S. Liu, B.-P. Zhang, J.-F. Li, L.-D. Zhao, J. Phys. D: Appl. Phys. 40, 566 (2007).

9. C. Recknagel, N. Reinfried, P. Höhn, W. Schnelle, H. Rosner, G. Yu, A. Leithe-Jasper, Sci. Technol. Adv. Mater. 8, 357 (2007).

10. J. X. Zhang, Q. M. Lu, K. G. Liu, L. Zhang, M. L. Zhou, Mater. Lett. 58, 1981 (2004).

11. D. Kenfaui, B. Lenoir, D. Chateigner, B. Ouladdiaf, M. Gomina, J.G. Noudem, J. Eur. Cer. Soc. 32, 2405 (2012).

12. S.D. Bhame, D. Pravarthana, W. Prellier, J.G. Noudem, Appl. Phys. Lett. 102, 211901 (2013).

13. W. Xie, J. He, S. Zhu, T. Holgate, Sh. Wang, X. Tang, Q. Zhang, T.M. Tritt, J. Mater. Res. 26, 1791 (2011).

14. Q. Lognoné, F. Gascoin, O.I. Lebedev, L. Lutterotti, S. Gascoin, D. Chateigner, J. Amer. Ceram. Soc., 97, 2038 (2014).

15. X. Yan, B. Poudel, Y. Ma, W.S. Liu, G. Joshi, H. Wang, Y. Lan, D. Wang, G. Chen, Z.F. Ren, Nano Lett. 10, 3373 (2010).

16. T. Caillat, M. Carle, P. Pierrat, H. Scherrer, S. Scherrer, J. Phys. Chem. Solids 53, 1121 (1992).

17. Y. Zheng, Q. Zhang, X. Su, H. Xie, Sh. Shu, T. Chen, G. Tan, Y. Yan, X. Tang, C. Uher, G.J. Snyder, Adv. Energy. Mater. 5, 1401391 (2014).

Figure captions

Fig. 1 Schematic diagram for the arrangement of the a) grinded sample; b) aligned sample in the SPS die.

Fig. 2 XRD patterns obtained from the polished bulk a) aligned (blue colour) and grinded (red colour) samples of $Sb_{1.48}Bi_{0.52}Te_3$; b) single SPS (red colour) and double SPS (blue colour) samples of $Sb_{1.5}Bi_{0.5}Te_{3.1}$. The main diffracting planes of the structure are mentioned in brackets above each pair of samples.

Fig. 3 SEM fracture images of a) grinded sample and b) aligned sample of $Sb_{1.52}Bi_{0.48}Te_3$ taken perpendicular to the pressing direction. The scale bar corresponds to 20 μm.

Fig. 4 SEM fracture images of a) single SPS and b) double-SPS $Sb_{1.6}Bi_{0.4}Te_{3.1}$ samples taken along the pressing direction of SPS. The scale bar corresponds to 20μm.

Fig. 5 Temperature dependence of (a) electrical resistivity, (b) thermopower, (c) hole concentration, (d) Hall mobility, (e) total thermal conductivity and (f) *ZT* of MS $Sb_{1.52}Bi_{0.48}Te_3$ grinded (grey half-filled square symbol), aligned (orange-filled square symbol) and reference (green open circle symbol). Measurements were performed along the direction perpendicular to the pressing direction.

Fig. 6 Temperature dependence of (a) electrical resistivity, (b) thermopower, (c) hole concentration, (d) Hall mobility, (e) total thermal conductivity and (f) *ZT* of reference and MS $Sb_{1.5}Bi_{0.5}Te_{3.1}$ single SPS (light-blue filled round symbol), double-SPS (black filled square symbol) and reference (red open circle symbol) samples. Measurements were performed along the direction perpendicular to the pressing direction.

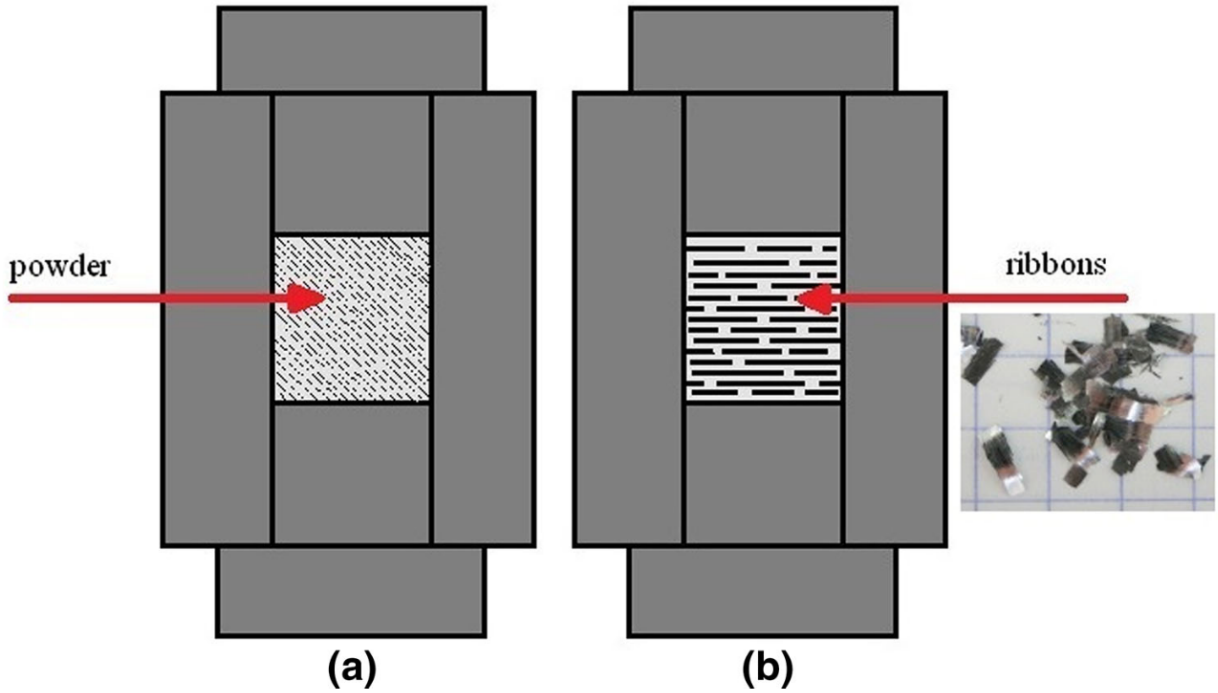

Figure 1

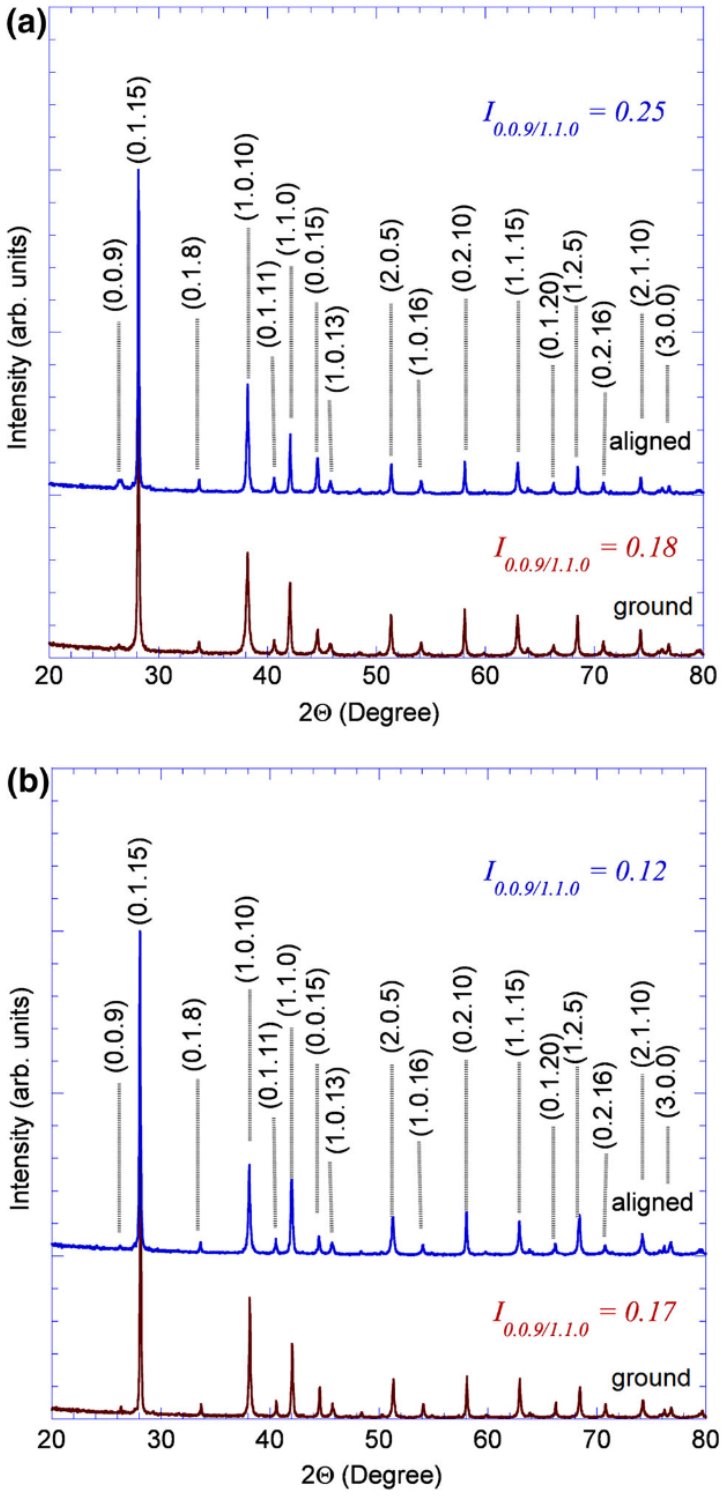
(a)
$I_{0.0.9/1.1.0}$ = 0.25
(0.0.9)
(0.1.15)
(0.1.8)
(1.0.10)
(0.1.11)
(1.1.0)
(0.0.15)
(1.0.13)
(2.0.5)
(1.0.16)
(0.2.10)
(1.1.15)
(0.1.20)
(1.2.5)
(0.2.16)
(2.1.10)
(3.0.0)
aligned
$I_{0.0.9/1.1.0}$ = 0.18
ground
Intensity (arb. units)
20
30
40
50
60
70
80
2Θ (Degree)
(b)
$I_{0.0.9/1.1.0}$ = 0.12
(0.0.9)
(0.1.15)
(0.1.8)
(1.0.10)
(0.1.11)
(1.1.0)
(0.0.15)
(1.0.13)
(2.0.5)
(1.0.16)
(0.2.10)
(1.1.15)
(0.1.20)
(1.2.5)
(0.2.16)
(2.1.10)
(3.0.0)
aligned
$I_{0.0.9/1.1.0}$ = 0.17
ground
Intensity (arb. units)
20
30
40
50
60
70
80
2Θ (Degree)

Figure 2

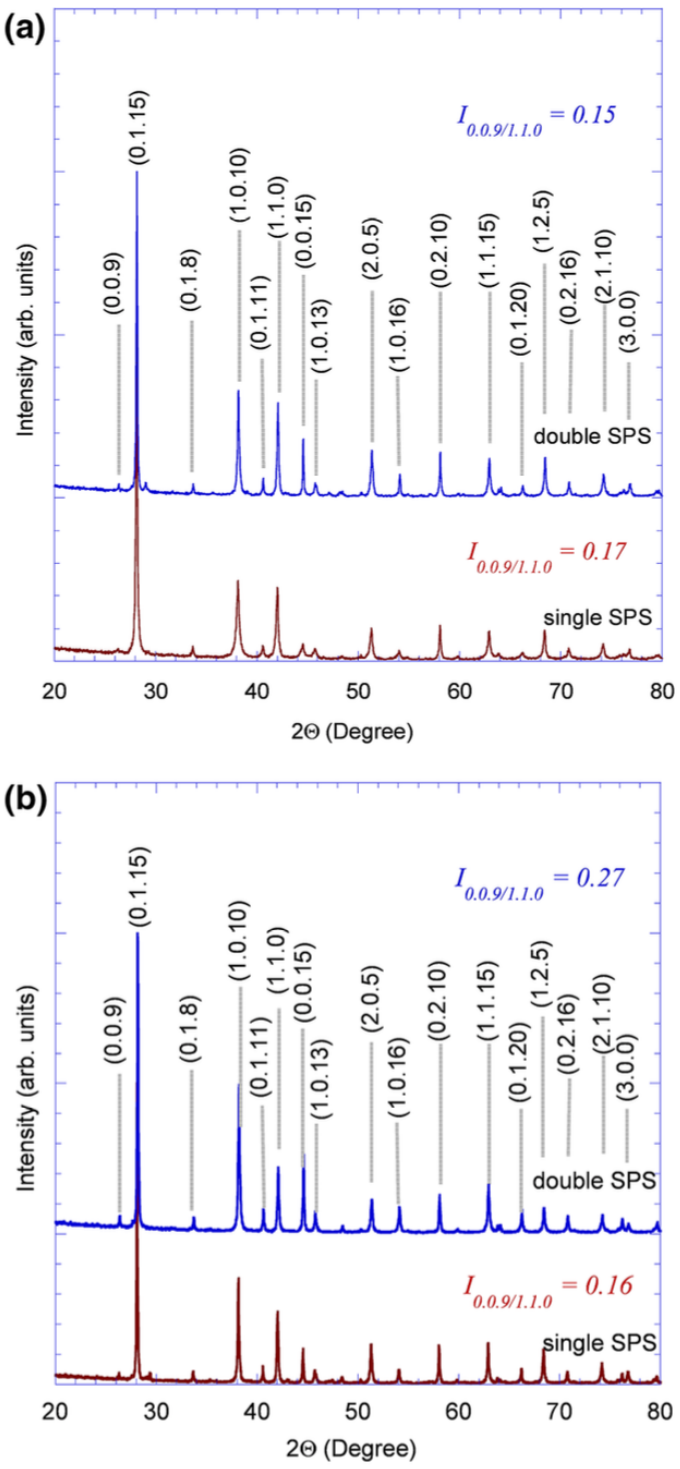
(a)
$I_{0.0.9/1.1.0}$ = 0.15
(0.0.9)
(0.1.15)
(0.1.8)
(1.0.10)
(0.1.11)
(1.1.0)
(0.0.15)
(1.0.13)
(2.0.5)
(1.0.16)
(0.2.10)
(1.1.15)
(0.1.20)
(1.2.5)
(0.2.16)
(2.1.10)
(3.0.0)
double SPS
$I_{0.0.9/1.1.0}$ = 0.17
single SPS
Intensity (arb. units)
20
30
40
50
60
70
80
2Θ (Degree)
(b)
$I_{0.0.9/1.1.0}$ = 0.27
(0.0.9)
(0.1.15)
(0.1.8)
(1.0.10)
(0.1.11)
(1.1.0)
(0.0.15)
(1.0.13)
(2.0.5)
(1.0.16)
(0.2.10)
(1.1.15)
(0.1.20)
(1.2.5)
(0.2.16)
(2.1.10)
(3.0.0)
double SPS
$I_{0.0.9/1.1.0}$ = 0.16
single SPS
Intensity (arb. units)
20
30
40
50
60
70
80
2Θ (Degree)

Figure 3

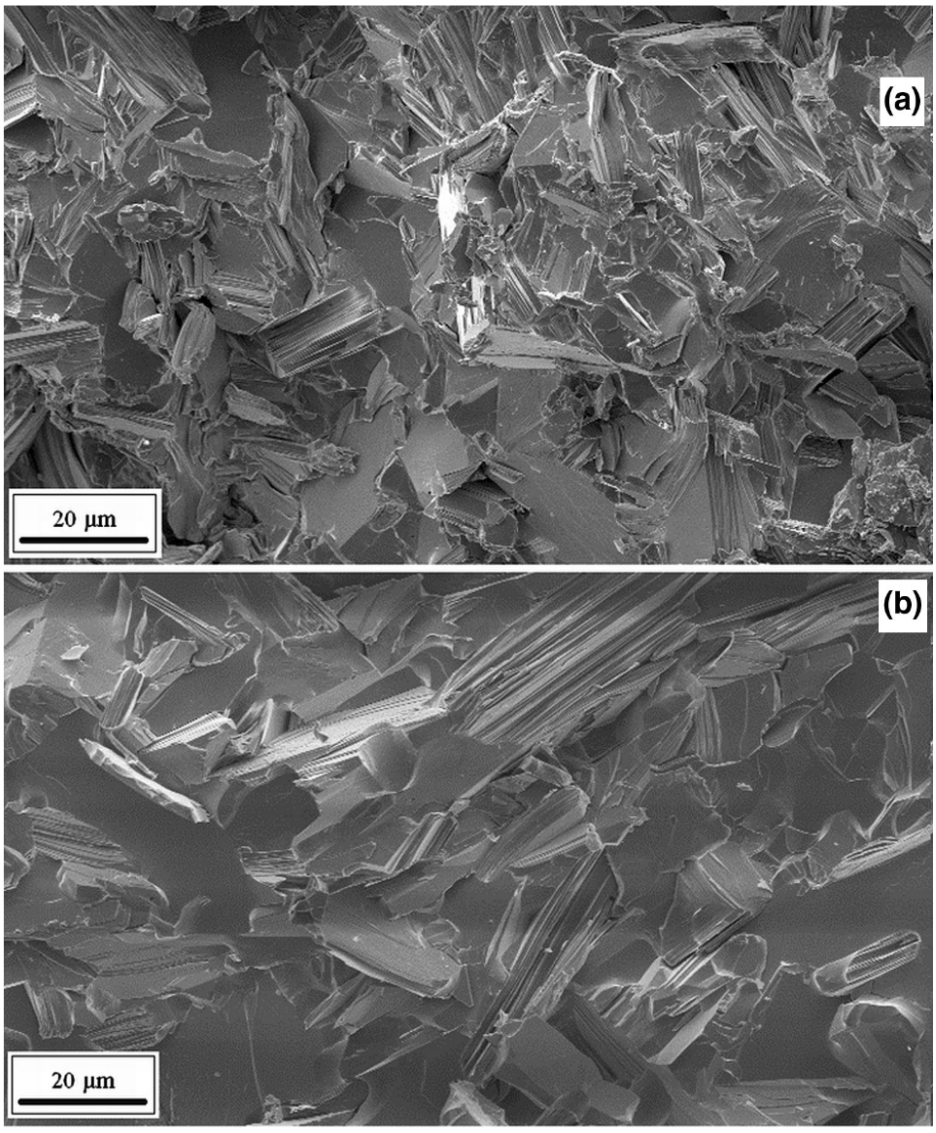

Figure 4

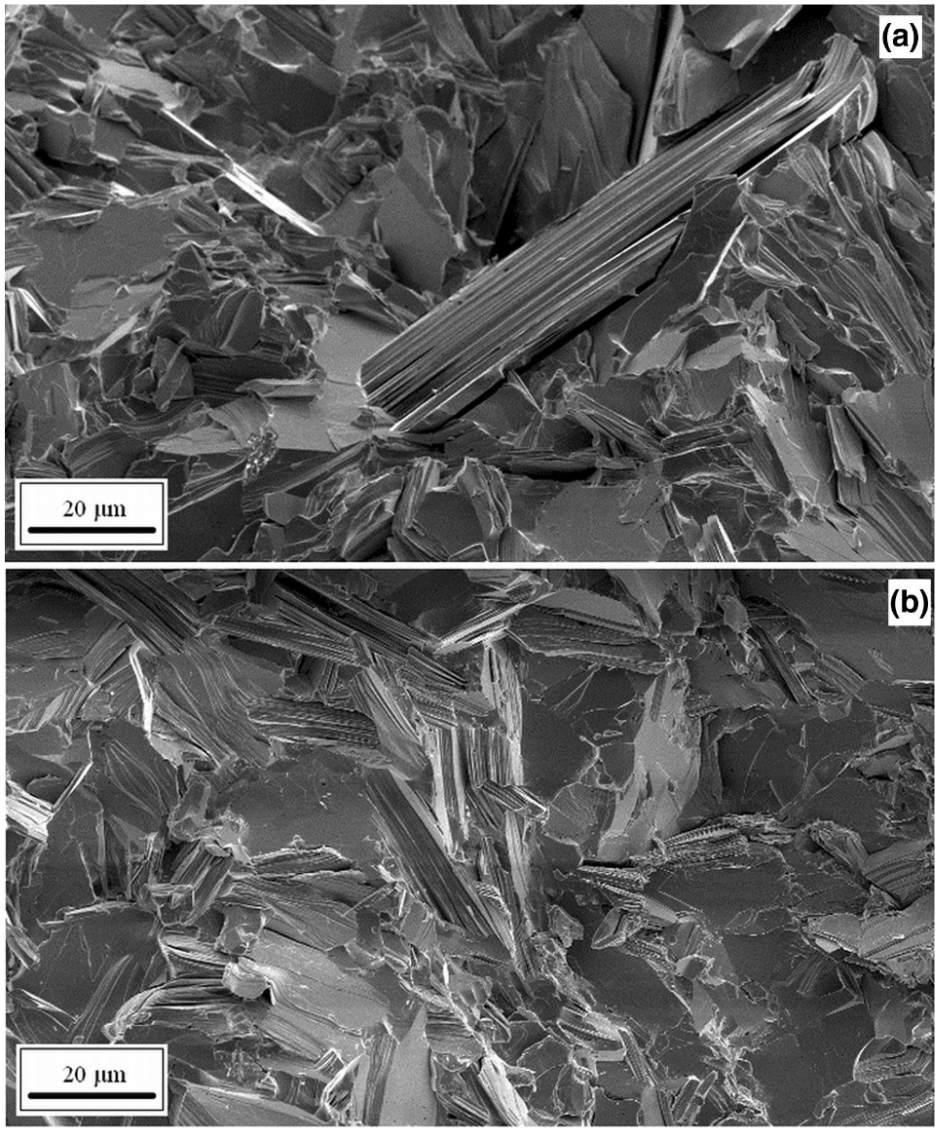

Figure 5

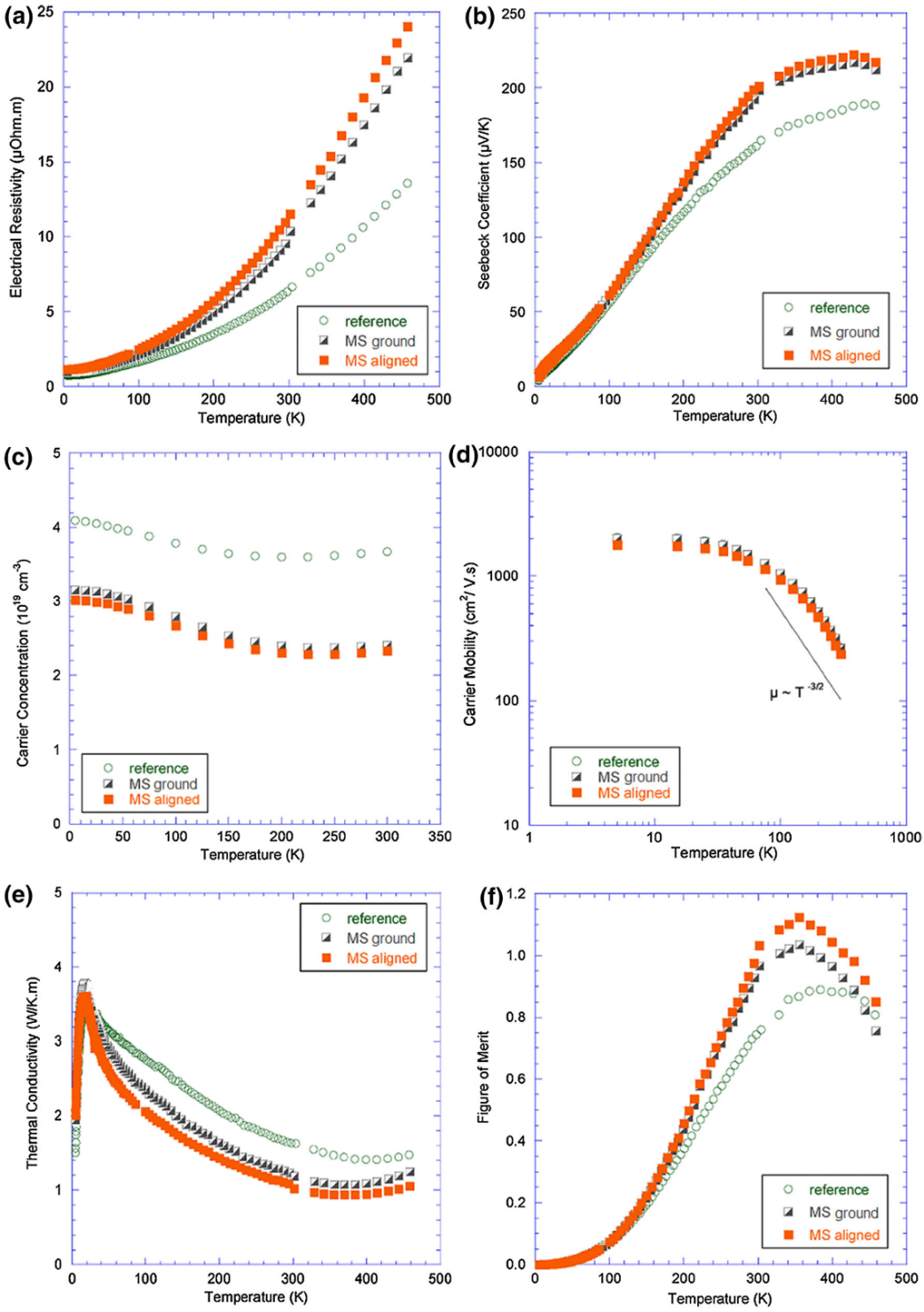
(a)
Electrical Resistivity (μOhm.m)
Temperature (K)
reference
MS ground
MS aligned
(b)
Seebeck Coefficient (μV/K)
Temperature (K)
reference
MS ground
MS aligned
(c)
Carrier Concentration (10^{19} cm^{-3})
Temperature (K)
reference
MS ground
MS aligned
(d)
Carrier Mobility (cm^2/ V.s)
$\mu \sim T^{-3/2}$
Temperature (K)
reference
MS ground
MS aligned
(e)
Thermal Conductivity (W/K.m)
Temperature (K)
reference
MS ground
MS aligned
(f)
Figure of Merit
Temperature (K)
reference
MS ground
MS aligned

Figure 6